

FEEP Thruster Survivability in the LEO Atomic Oxygen Environment

Fabio Ceccanti, Salvo Marcuccio, Mariano Andrenucci
Centrosazio - Alta S.r.l.
Via Gherardesca 5, 56014 Ospedaletto, Pisa, Italy
Tel. +39 050 985072
f.ceccanti@alta-space.com

IEPC-01-295

In FEEP thrusters, field ionisation of propellant, usually cesium, occurs on the liquid metal surface at the outlet of a micrometric slit. Some concern was raised on the use of FEEP in low Earth orbit, since it was feared that the relatively high atomic oxygen concentration could provoke clogging of the slit due to cesium oxidation. To assess this potential failure mechanism we have investigated the FEEP thruster compatibility with a 200 km altitude atomic oxygen environment. In our experiment, a 50 mm slit, 1 mN FEEP thruster was exposed to direct impingement of atomic oxygen. Ion emission quality was monitored using scanning electrostatic probes. No significant degradation of the thruster performance was observed after as long as 384 hours total exposure to severe atomic oxygen flux and to an intense molecular oxygen background. It is concluded that the FEEP thruster can survive in a very low LEO environment without failures due to interaction with the residual atmosphere.

Introduction

Orbit maintenance and attitude control of LEO (Low Earth Orbit) spacecraft are among the envisaged uses of FEEP (Field Emission Electric Propulsion) thrusters. While the majority of missions will be flown at relatively high altitudes, as for sun-synchronous satellites, some low altitude Earth orbiting spacecraft are foreseen as well, like e.g. the recently approved ESA mission GOCE (Gravity field and steady state Ocean Circulation Explorer). This mission, dedicated to a detailed survey of the Earth's gravitational field, will employ a 1000 kg-class, 4 m long, elongated spacecraft provided with a gridded ion engine to continuously counteract atmospheric drag. FEEP is a candidate technology for the 1 mN propulsion assembly that shall provide drag compensation and attitude control along the axes transvers with respect to orbital velocity. Due to the stringent requirements posed by the scientific goals, GOCE will fly in a very low circular orbit, nominally at about 250 km, with a worst-case safe-mode operational altitude as low as 200 km.

Thrust production in a FEEP thruster is based on ionisation and acceleration of a liquid metal propellant

that occurs at the outlet of a micrometric slit. The propellant of choice is cesium, due to the fact that it has a low melting temperature, the lowest ionisation potential among all elements, low surface tension, high atomic mass, and a number of other favourable physical properties. The main concern raised in the past on the slit-emitter ionisation mechanism was the possible clogging of the emitter slit due to oxidation of cesium. As an alkali metal, cesium reacts with water and with oxygen, forming a number of compounds with high melting or decomposition temperature. It was feared that, at the normal operating temperature of FEEP (about 35 °C), contamination by oxides could result in partial obstruction of the slit by solid particles, leading to poor ion emission or even complete failure. This situation could take place because of interaction of the free liquid metal surface at the emitter slit with the external atmosphere. Clearly, this concern regards the use of FEEP in low Earth orbit, where the atmosphere is denser and richer in oxygen.

Since the main atmospheric constituent in LEO is atomic oxygen, it was deemed appropriate to assess this potential failure mechanism with a direct experimental approach by exposing the thruster to an

atomic oxygen flux representative of the very low Earth orbit environment (this test will be referred to in the following as “Atox test”). To accomplish this goal, first a atomic oxygen source was designed and built; a suitable set of probes was used to characterise the atomic oxygen beam; the source was integrated into one of the FEEP test facilities at Centropazio; and finally, the exposure test was performed. The GOCE mission scenario was considered as the reference case.

In this paper, an overview of the environmental conditions in LEO is given, followed by a summary of previous results concerning the interactions of cesium

with atmospheric constituents in FEEP. The atomic oxygen source and the related experimental apparatus is described, and the results of the exposure test on a 50 mm slit, 1 mN-class thruster are reported.

LEO Environment and Reference Condition

At the reference 200 km altitude, residual atmosphere is primarily composed of atomic oxygen (O) and molecular nitrogen (N₂), with a minor contribution of molecular oxygen (Table 1). No significant interaction with atmospheric molecular nitrogen is reported in literature referring to cesium exposure to air, with a

Table 1. Atmospheric composition at 200 km

Species	Molec. mass	Number density (cm ⁻³)		Number density %		Mass density (g/cm ³)		Mass density %	
		(a)	(b)	(a)	(b)	(a)	(b)	(a)	(b)
Ar	40	4.0·10 ⁶	1.4·10 ⁷	0.04%	0.16%	2.67·10 ⁻¹⁶	9.35·10 ⁻¹⁶	0.07%	0.25%
H	1	8.0·10 ⁴	5.0·10 ⁴	0.00%	0.00%	1.34·10 ⁻¹⁹	8.35·10 ⁻²⁰	0.00%	0.00%
He	4	1.5·10 ⁷	1.0·10 ⁶	0.15%	0.01%	1.00·10 ⁻¹⁶	6.68·10 ⁻¹⁸	0.03%	0.00%
N	14	5.0·10 ⁷	3.0·10 ⁷	0.48%	0.35%	1.17·10 ⁻¹⁵	7.014·10 ⁻¹⁶	0.32%	0.19%
N ₂	28	4.0·10 ⁹	6.2·10 ⁹	38.7%	71.3%	1.87·10 ⁻¹³	2.90·10 ⁻¹³	51.9%	78.3%
O	16	6.0·10⁹	2.0·10 ⁹	58.0%	23.0%	1.60·10 ⁻¹³	5.34·10 ⁻¹⁴	44.5%	14.4%
O ₂	32	2.7·10 ⁸	4.5·10 ⁸	2.61%	5.18%	1.44·10 ⁻¹⁴	2.40·10 ⁻¹⁴	4.01%	6.5%
Total		1.03·10 ¹⁰	8.07·10 ⁹			3.6·10 ⁻¹³	3.7·10 ⁻¹³		
Local temperature (K)						970	1220		
Total pressure (mbar)						1.39·10 ⁻⁶	1.47·10 ⁻⁶		

(a) Data at maximum local atomic oxygen number density (lat. = 45°N, long. = 90°W).

(b) Data at minimum local atomic oxygen number density (lat. = 90°S, long. = 90°E).

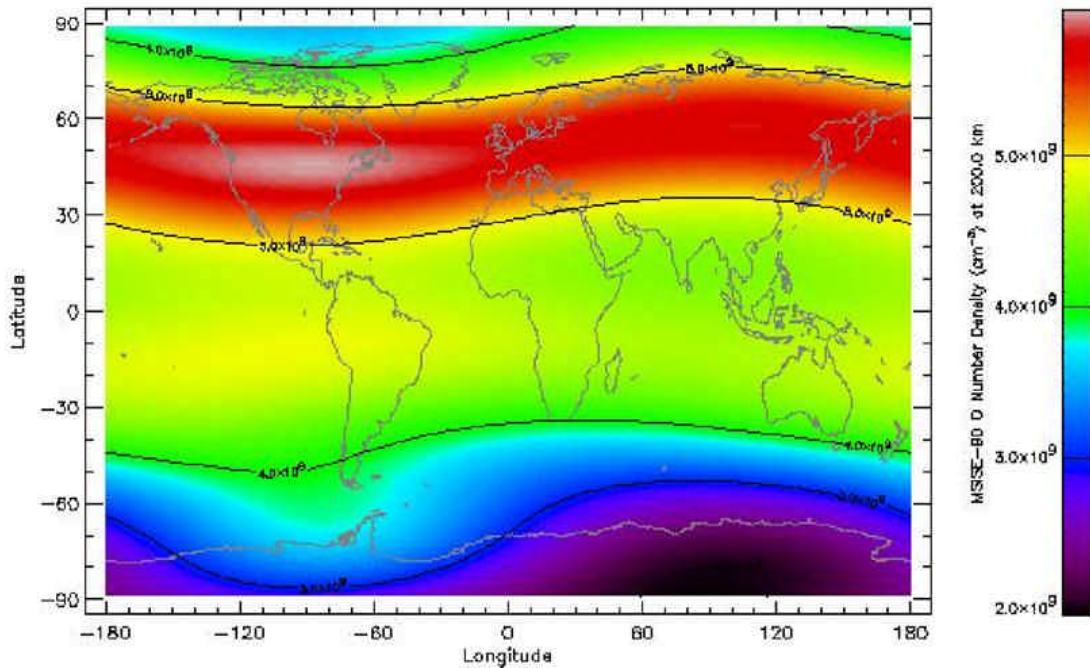


Figure 1 - Atmospheric composition at 200 km

Table 2. GOCE mission: operational modes and environmental conditions

	Mode A Satellite safe mode	Mode B Satellite measurement / maintenance mode
Altitude	200 km	240 km
Exposure time	25 days	30 months
AO flux (flight cond.)	$5.98 \cdot 10^{15} \text{ cm}^{-2} \text{ s}^{-1}$	$1.7 \cdot 10^{15} \text{ cm}^{-2} \text{ s}^{-1}$
Max. pressure	$1.8 \cdot 10^{-6} \text{ mbar}$	$1.8 \cdot 10^{-6} \text{ mbar}$
FEEP mode	OFF	ON, stand-by at minimum thrust
Impingement	Direct (thrust vector parallel to S/C velocity vector)	Tangential (thrust vector normal to S/C velocity vector)
AO flux on the slit (with safety margin)	$1.2 \cdot 10^{16} \text{ cm}^{-2} \text{ s}^{-1}$	$5.4 \cdot 10^9 \text{ cm}^{-2} \text{ s}^{-1}$
Temperature	ambient - 80 °C	ambient - 80 °C

high degree of confidence in this sense also given by previous test results ([1], [2]). Data in Table 1 have been obtained using the Mass Spectrometer Incoherent Scatter (MSISE-90) atmospheric model, developed by NASA's Goddard Space Flight Center. Data and plots have been obtained using the SPace ENVironment Information System (SPENVIS), an on-line tool provided by the ESA/ESTEC and the Belgian Institute for Space Aeronomy [3]. Simulations have been run on a world map coordinate grid, choosing maximum solar flux conditions and worst case local time (14:00 h). Simulation results for atomic oxygen number density are shown in Fig. 1. Figure 2 shows the atomic oxygen flux in LEO. At 200 km altitude, a maximum impinging flux of up to $3.6 \cdot 10^{15}$ atoms/cm²·s is envisaged.

The reference condition assumed for the Atox test is derived from the GOCE requirements. The specifications for the GOCE mission define two different operational modes, related to different environmental conditions and described in Table 2. Environmental conditions, in the case of mode A, are

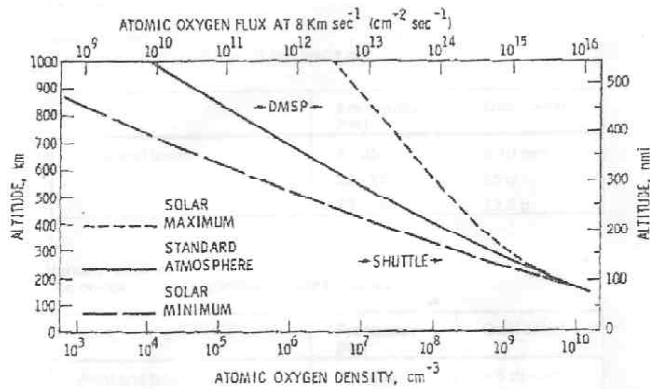


Figure 2 - Atmospheric Atomic Oxygen density in Low Earth Orbit (from [12])

worst case in any respect (atomic oxygen local density, impingement type, FEEP operational mode) and have been taken as reference conditions. Exposure time is higher in operational mode B than in mode A, but the total amount of oxygen impinging the slit is five orders of magnitude lower, due to the angle between the thruster and the orbital velocity vector.

Previous Test Results

Experimental characterization of cesium fed FEEP thrusters with specific consideration of the effects of the ambient pressure has been performed by Mitterauer [1] and by Genovese et al. [2]. At the University of Vienna, Mitterauer observed slit clogging after a 60 days thruster switch-off period in a residual atmosphere at about $5 \cdot 10^{-9}$ mbar total vacuum with a 6% H₂O content. It is believed that clogging was mainly due to formation of cesium hydroxide. Normal operating conditions could be restored by imposing a slightly positive pressure in the cesium feeding by means of a mechanical pump. Emission started "... from several distinct emission sites originating from localized mechanical penetration of the solid crust of contaminations at the emitter slit orifice" [1]. After some continuous emission, full reconditioning was obtained, showing to a good extent the self-decontaminating properties of the linear slit emitter.

The test campaign conducted at Centropazio [2] showed that the thruster performance is unaffected by operation at a background pressure higher than that expected for the GOCE reference condition, as "no appreciable effect on emitter performance appeared until pressure reached 10^{-4} mbar". This value is two orders of magnitude greater than that

reported in Table 1. During the same campaign, the effect of prolonged shut-off thruster exposure to high background pressure conditions was also investigated. After a 15 hours period in a 10^{-4} mbar environment, “the thruster was easily ignited at the first attempt, but the threshold voltage was slightly larger than in previous case (7.3 kV)...Threshold voltage reverted to 6.9 kV a few minutes after, when the impurities were blown away and good slit wetting condition was established again” [2].

Recent observations at Centropazio and at the Electric Propulsion Laboratory of the European Space Agency have shown that the thruster tolerates exposure to a background pressure as high as 10^{-2} mbar for about 10 hours. In both cases, cesium-fed emitters were unintentionally exposed to such a unfriendly environment due to occasional black-outs of the unattended vacuum facility pumping system during the night. As nominal vacuum was restored, the thrusters were restarted and brought back to normal operation after a short recovery procedure consisting in heating at about 60 °C for a few tens minutes.

Finally, at the end of a recent series of tests at Centropazio on a 50 mm linear slit cesium fed FEEP emitter, the thruster was restarted after exposure to laboratory ambient air consequent to the opening of the vacuum chamber. In this very extreme case, ion emission along a portion of the slit was obtained after heating at about 100 °C for one hour. Due to other impending activities on the same facility, no further attempt was made to investigate the possibility of full recovery.

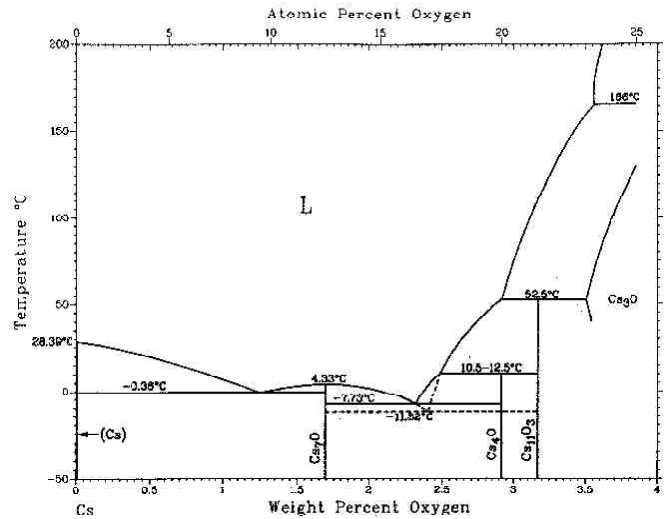


Figure 3 - Cesium-Oxygen phase diagram [4]

Cesium-Oxygen Interactions

Cesium is the most alkaline and electropositive of all elements. It reacts explosively with water to form cesium hydroxide, the strongest base known, and reacts with ice at temperatures above -116°C. In air, cesium reacts readily with molecular oxygen and moisture. Although most available literature (refs. [5], [6] and [7]) refers to the interaction between cesium and molecular oxygen, the same variety of cesium-oxygen compounds may be expected from the cesium-atomic oxygen reaction. A list of cesium oxides and their properties is reported in Table 3, containing data

Table 3. Properties of Cesium oxides

Name	Formula	Melting temp. (decomposition)	Color	Crystal structure
Heptacesium oxide	Cs ₇ O or [Cs ₁₁ O ₃]Cs ₁₀	4.3° C (dec. in liq. phase into LCs and Cs ₃ O)	Bronze	hexagonal
Tetracesium oxide	Cs ₄ O	(d = 12.5 ° C)	Golden	
Endecacesium trioxide	Cs ₁₁ O ₃	(d = 52.5 ° C)		
Heptacesium dioxide	Cs ₇ O ₂	(d = 50 ° C)	Violet	
Tricesium oxide	Cs ₃ O	(d = 166 ° C)	Black	hexagonal
Cesium oxide	Cs ₂ O	490° C (d = 700° C)	Yellow / red / black	rombohedral
Cesium peroxide	Cs ₂ O ₂	594° C (d = 650° C)	Yellow / brown	orthorombic
Sesquicesium oxide	Cs ₂ O ₃	502° C (d = 850° C)	Black	centered cubic
Cesium superoxide	CsO ₂	433° C (d = 880° C)	Orange	square
Cesium ozonate (Cesium trioxide)	CsO ₃	Unstable, decomposes with release of oxygen	Bright red	

extracted from ref. [6], [7] and [8]. The most common cesium-oxygen binary compounds are cesium superoxide, CsO_2 , that results if cesium is burned in air, cesium oxide, Cs_2O , and cesium peroxide, Cs_2O_2 .

In the case of FEEP, a liquid or solid surface of pure cesium metal is impinged by a stream of atomic oxygen. It is well known from the literature that oxygen is extremely soluble in cesium up to medium-high concentrations. The Cs-O phase diagram up to oxygen atomic percent of 25% is reported in figure 3. From this diagram and the data in Table 2 we can derive the following considerations:

- up to an atomic percentage of about 18%, the solution melting point is below that of pure cesium;
- up to an atomic percentage of about 23%, the solution can be melted at temperatures below 166° ; in these conditions, the liquid solution is basically composed by a mixture of liquid cesium and Cs_3O , the only cesium oxide in this range that doesn't dissociate below melting temperature;
- at higher oxygen concentrations, the solution melting point rises to 490°C at 33% (Cs_2O) and 594°C at 50% (Cs_2O_2), then decreases again to 433°C at 66% (CsO_2);
- beyond this concentration, no further increase of oxygen content is tolerated by mixture, and additional oxygen is released in molecular form.

Chemical and Physical Parameters

The knowledge of the Cs-O system behaviour alone is not sufficient to fully predict the situation on the FEEP emitter slit. A detailed theoretical analysis of the behaviour of the cesium meniscus under the expected atomic oxygen flux is complicated by the large amount of chemical and physical phenomena involved, a brief description of which is reported in the following.

Multiphase equilibrium and solubility

Depending on temperature and composition, many different phases can be present at the same time. Neglecting contribution of local atmosphere of evaporated species in front of the slit, cesium metal together with a number of oxygen compounds between those illustrated in figure 3 and table 3 can be present either in solid or liquid phase. A certain amount of solute nitrogen (N_2) or nitrogen compounds such as cesium azide (CsN_3) could also be present, even if as a minor contribution. Due to the atmospheric composition, the presence of other compounds such as cesium hydride (HCs) can be neglected. No

conclusive data is available on solubility of cesium oxides in melted cesium, formation of oxide crystals on the liquid metal surface and cohesion of these crystals.

Diffusion

From figure 3 we derive that slit clogging can happen only if local oxygen concentration is higher than a certain value enabling all cesium to be "trapped" in oxygen compounds melting at high temperature, such as cesium oxide (Cs_2O). When cesium is in the liquid phase, a certain diffusion rate of oxygen atoms is expected, thus reducing local oxygen concentration. As no data on diffusivity of oxygen or cesium oxides in melted cesium could be found in literature, no analytical provisions can be made on this subject. On the opposite side, when cesium is in solid phase, diffusivity is expected to be very slow, and clogging concentration can be reached more easily. While this can be considered a negative aspect, it is nevertheless quite probable that the formation of a solid oxide crust can prevent further absorption of oxygen. Furthermore, there is no information on the behaviour of this crust when the metallic cesium behind is melted.

Velocity of impinging particles

Cesium reacts or solutes oxygen very easily. No possibility to repel impinging oxygen (whether atomic or molecular) is foreseen, therefore the velocity of impinging particle is essentially unimportant to the end of the kinetics of the combinative phenomena. On the other hand, the depth of penetration of oxygen atoms will be strongly influenced by their energy. Clearly, deeper mean penetration results in lower local concentration. A lower particle velocity (as during the Atox test, with respect to actual flight conditions) can therefore be considered an aggravating factor with respect to the potentially induced rate of oxydation. Moreover, high-energy atoms impinging on the oxide crust could produce back sputtering of contaminants, and therefore alleviate the effective slit clogging.

Field emission

During normal thruster operation, the ejected propellant mass per unit time is given by:

$$\dot{m}_p = \frac{T}{g_0 I_{sp}}$$

where T is thrust level, g_0 is the gravity constant and I_{sp} is the thruster specific impulse. The minimum propellant flux is given by minimum T and maximum

I_{sp} . The minimum required thrust for most FEEP applications is about 1 μ N, while I_{sp} can be, for cesium, as high as 10000 s. The minimum cesium flux during operation is then in the order of:

$$(\dot{m}_p)_{\min} = 10^{-11} \text{ kg/s}$$

The minimum atomic cesium flux through the slit cross-section during operation is given by:

$$F_{Cs}^T = \frac{(\dot{m}_p)_{\min}}{L_{slit} h_{slit}} \frac{N_A}{M_{Cs}} = 7.5 \cdot 10^{16} \frac{\text{atoms}}{\text{cm}^2 \cdot \text{s}}$$

where L_{slit} and h_{slit} are slit dimensions, N_A is the Avogadro number and M_{Cs} is cesium atomic mass. Maximum cesium flux (at 1 mN) is about 1000 times higher. Being the ejected cesium quantity from 20 to 20,000 times larger than that of incoming atomic oxygen, no appreciable performance deterioration is expected during normal operation. Obviously, this does not apply when the thruster is switched off.

Evaporation

Ref. [9] gives the following expression for evaporation of a liquid metal into a vacuum:

$$\log W = A - B/T - 0.5 \log T + C$$

where T is the liquid surface temperature in K and W is expressed in $\text{g} \cdot \text{s} \cdot \text{cm}^{-2}$. For liquid cesium [9]:

$$\begin{aligned} A &= 9.86 \\ B &= 3774 \\ C &= -3.1722 \end{aligned}$$

Thus, for a typical thruster temperature of 35 °C:

$$W = 1.57 \cdot 10^{-7} \text{ g/cm}^2 \cdot \text{s}$$

The atomic flux is therefore given by:

$$F_{Cs}^E = \frac{W \cdot N_A}{M_{Cs}} = 7.11 \cdot 10^{14} \frac{\text{atoms}}{\text{cm}^2 \cdot \text{s}}$$

How this rate can interfere with formation of contaminants on the free surface is not easily quantifiable, but only positive effects are foreseen.

From all the considerations above, it is envisaged that worst exposure condition for the thruster is the one with thruster switched off and cold emitter (i.e. solid cesium). This assumption was confirmed by test results.

The Atomic Oxygen Source

The atomic oxygen source (Fig. 4) was designed and manufactured at Centropazio in cooperation with the

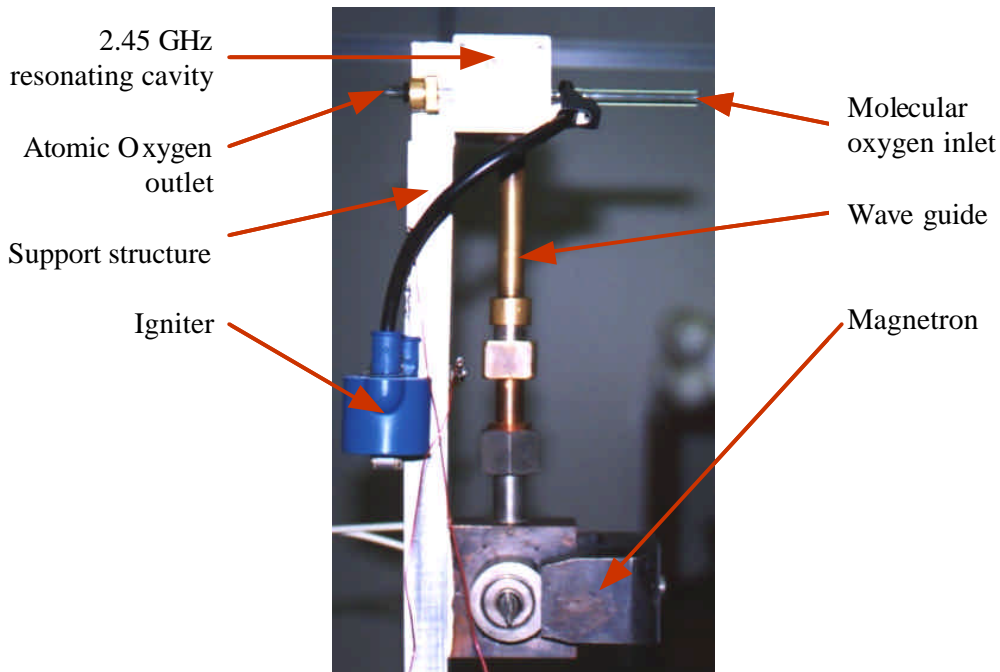


Figure 4 -The atomic oxygen source

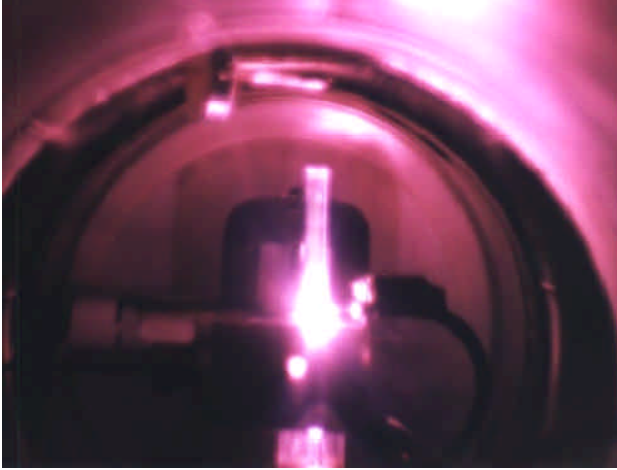


Figure 5 - The atomic oxygen source in operation.

Department of Physics of the University of Pisa. The source is based on a magnetron microwave oscillator and on a resonating cavity crossed by a quartz discharge tube where molecular oxygen dissociation takes place. The Philips 7090 magnetron voltage and current are controlled by a dedicated 220V, three-phase power supply. Generated electromagnetic power is then driven to the cavity by a coaxial wave guide, carefully designed to avoid microwave leakage or back reflection. The cavity has been designed to resonate at 2.45 GHz at 1/4 of wave ($\lambda/4 = 30.61$ mm) and can be fine-tuned by adjusting two screws. The discharge tube, with an inner diameter of 6 mm, is connected on one side to the molecular oxygen tank by proper tubes, fittings, valves and feedthroughs. In the tube, molecular oxygen crossing the resonating cavity is superheated by interaction with the microwaves, and dissociates by collision. During tuned operation, a red-violet discharge is visible in the quartz tube (Fig. 5). When dissociation takes place, a free stream of atomic oxygen exits from the other end of the tube. Quartz has been chosen as a trade-off between low surface recombination activity and high operating temperature.

An igniter is also needed for the discharge to begin. This device is based on a coil that generates a spark close to the discharge tube exit upon a trigger command. The high bandwidth electromagnetic perturbation generated by the spark breaks the unstable equilibrium of the superheated molecular oxygen and initiates the discharge chain reaction. The source is supported by an aluminium structure, and is fixed on an aluminium baseplate, acting as a heat sink. The baseplate is fixed and thermally coupled to one of the vacuum chamber blank flanges that can be thermally controlled from the outside of the chamber.

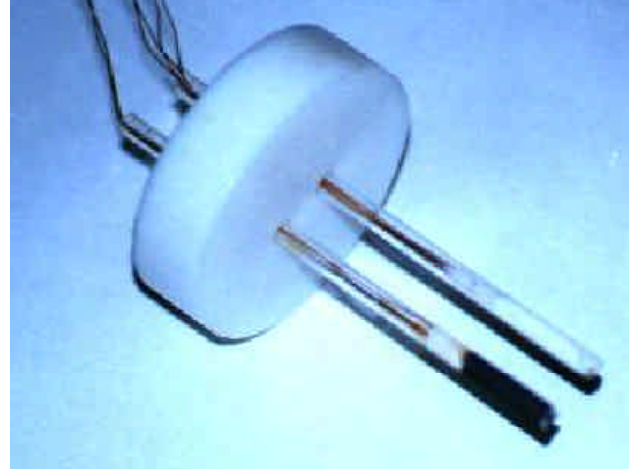


Figure 6 - Atomic oxygen flux measurement probe

Measurement of Atomic Oxygen Flux

The main parameter characterizing the source is the atomic oxygen flux (defined as the number of atoms per unit surface per unit time, and measured here in $\text{cm}^{-2} \text{s}^{-1}$) at a given distance from the discharge tube exit. A measure of the neutral atomic oxygen local flux has been made using a specifically designed equipment, based on the working principles defined in [10]. The measuring probe, shown in fig. 6, is composed of two parallel Pyrex tubes (50 mm long, external diameter 4 mm, internal diameter 2.5 mm) and a PTFE support structure. The first tube (tube No. 1) contains a platinum resistance (Pt100) for temperature sensing and is covered on the outside by a thin silver film (560 nm), obtained by vacuum deposition. The other tube (tube No. 2) is not silver coated, and contains a thick film resistor (1 kOhm) heater together with an identical Pt100 platinum resistance.

The probe working principle is based on the recombination activity of oxygen atoms on different surfaces. We define the *recombination coefficient*, K , as

$$K = \frac{N_{Or}}{N_O}$$

where N_{Or} is the number of recombinations and N_O is the number of atoms hitting the surface. After a few seconds of operation in the atomic oxygen environment, a film of silver oxide (AgO) forms on the surface of tube No. 1. Silver oxide is a very good catalyst for atomic oxygen recombination reactions, thus $K = 1$ can be assumed in this case. On the other hand, recombination on Pyrex is negligible [11], thus $K = 0$ can be assumed for tube No. 2. Both

assumptions are conservative, as they lead to an underestimate of the atomic oxygen flux.

Atoms hitting the silvered surface react forming oxygen molecules and releasing the binding energy, equal to 5.2 eV. This energy rises the tube temperature, and this rise is measured by the Pt100 sensor. No heating by this process is caused to tube No. 2. This tube is kept at the same temperature as tube No. 1 by adjusting the power provided to the internal heater. When the two tubes reach the same equilibrium temperature, the energy provided to the heater (a measured parameter) is equal to the energy deriving from the recombination reaction. The atomic oxygen flux is therefore given by:

$$F = \frac{2V_h I_h}{E \cdot \mathbf{f}_{ext} \cdot L_{Ag}}$$

where F is local atomic oxygen flux, V_h and I_h are respectively heater voltage and current (measured), E is O_2 molecular binding energy, and $\mathbf{f}_{ext} \cdot L_{Ag}$ is the silvered surface projected normal to flux direction (tube diameter times length of silver coating). Since the heater resistance is slightly variable with temperature, both heater tension and current were monitored.

Source performance

An extensive test campaign was conducted to characterize the atomic oxygen source performance both at the Department of Physics of the University of Pisa and at Centospazio. The atomic oxygen flux was measured at different distances from the source exit, and in different source operating conditions, namely:

- molecular oxygen mass flow, regulated by a precision leak valve and measured indirectly by the equilibrium chamber pressure, assuming constant pumping speed from the vacuum system;
- magnetron anodic current, determining generated electromagnetic power;
- magnetron (and therefore source) temperature.

Atomic oxygen flux showed, as expected, an inverse square correlation with distance and a linear correlation with mass flow, in the range 10^{-7} to 10^{-6} kg/s. Correlation with magnetron temperature was also linear in the range 30 to 110 °C. This was probably due more to modification of resonating chamber geometry (dependent also on the initial set-up of regulating screws) than to heat transfer phenomena. Temperature was never raised above 110 °C, to avoid the risk of damaging the magnetron.

The most interesting correlation, however, is that with the magnetron current. One example is given in figure 7, obtained in operating conditions equal to those of the compatibility test. At constant mass flow, the atomic oxygen flux increases with current with a typical saturation curve. When the plateau is reached, the percentage of dissociated oxygen is around 100%. This condition is confirmed by a brilliant red discharge. Rising magnetron current only determines a higher discharge temperature.

Atomic Oxygen Compatibility Test

Background

The Atox test was carried out on a 1 mN, 50 mm slit FEEP thruster operated with cesium propellant (Fig. 8). During August 2001, the thruster had undergone a characterization phase to assess its performance before starting of the Atox test. Fig. 9 shows the

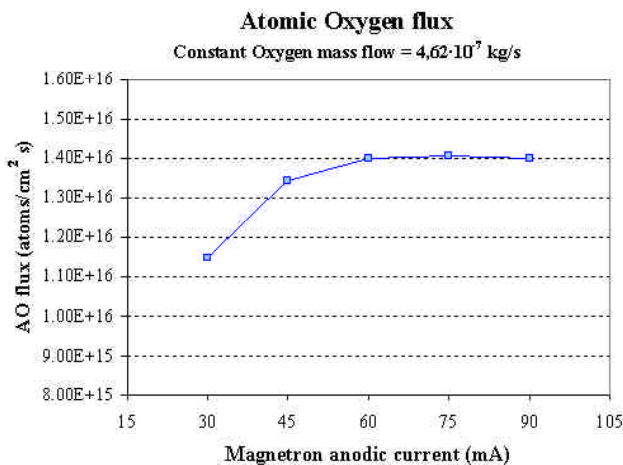


Figure 7 - Atomic Oxygen flux vs. magnetron current

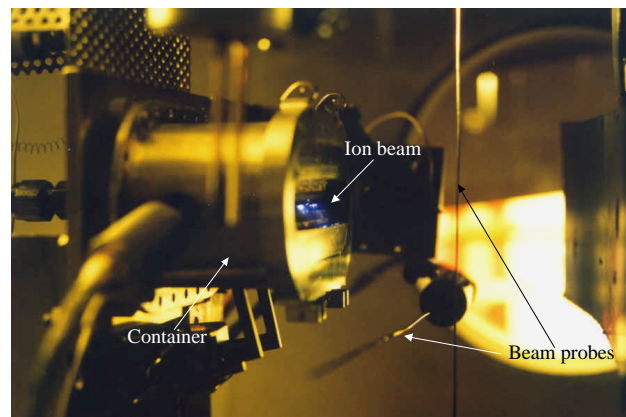


Figure 8 - The 1 mN FEEP thruster firing prior to Atox test

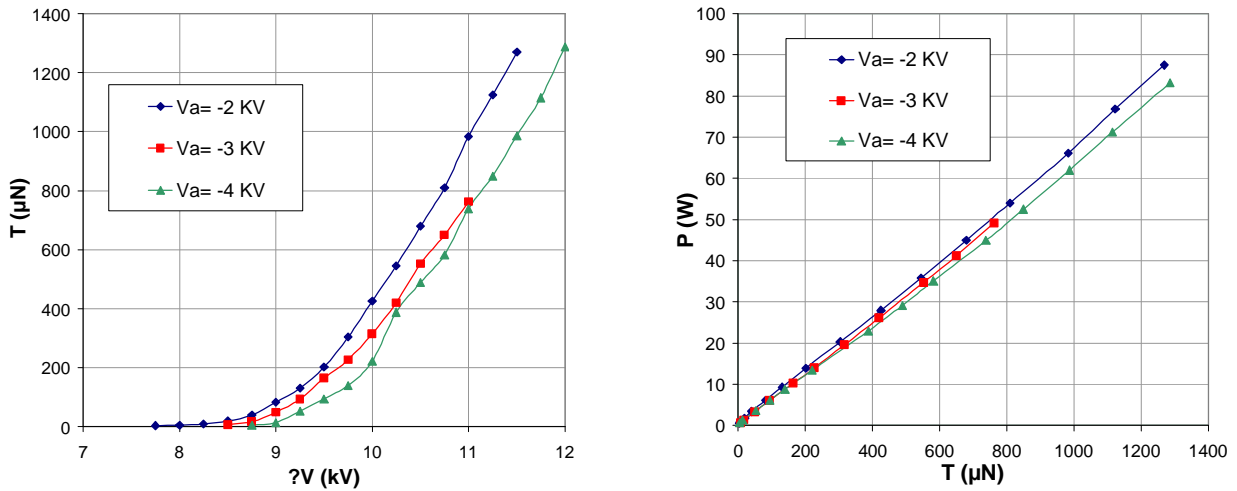


Figure 9 - Thruster performance curves: left, thrust vs. total electrode voltage; right, emitter power consumption vs. thrust. V_a is the accelerator voltage.

measured thrust vs. voltage and power vs. thrust curves. Thrust reduction due to beam divergency as been account for, as well as the power loss due to accelerator drain current.

The Atox test was performed in the IV1 Ultra High Vacuum facility of Centropazio/Alta, a stainless steel cylinder 0.6 m in diameter and 1.7 m long, allowing an ultimate vacuum of about 10^{-9} mbar. To match worst operating conditions as accurately as possible, the source was mounted directly in front of the thruster, with the atomic oxygen outlet facing the emitter slit center at a distance of about 15 cm. A simplified representation of test setup is given in figure 10, showing the relative position of the atomic oxygen source and the thruster. A shield/probe system was mounted on a rotatable arm controlled from outside of

the vacuum chamber, allowing the atomic oxygen probe to be immersed in the Atox stream to measure the flux or, alternatively, to insert a protective surface between the source and the thruster thus avoiding direct ion beam impingement on the source.

Ion beam probes

The ion beam current distribution was evaluated using a set of two single-filament Langmuir probes, made of 0.8 mm diameter stainless steel wires, 20 cm long, mounted on an isolating support. Probes are moved by two stepper motors to scan horizontally and vertically the ion beam, collecting a current roughly proportional to the incoming ion energy flux integrated along the probe length. The horizontal probe gives information about the ion beam main divergency angle, that is the beam aperture in a plane perpendicular to

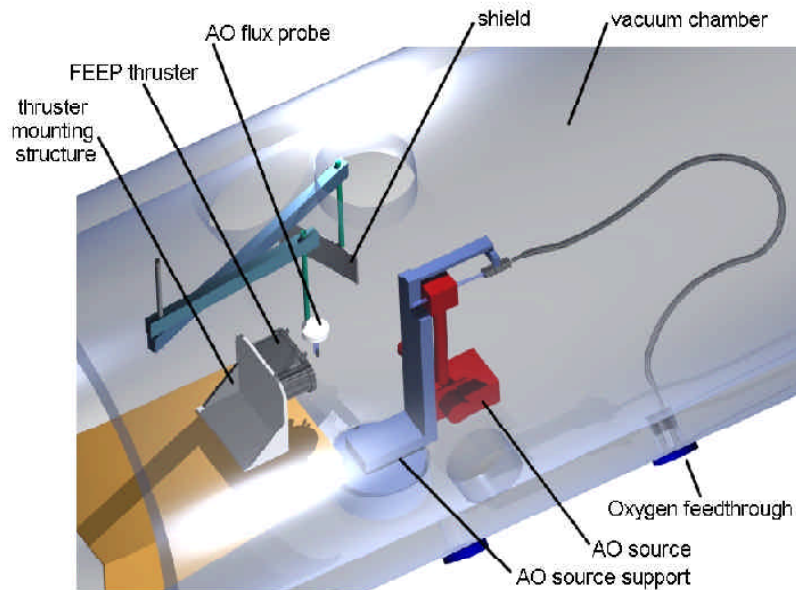


Figure 10 - Schematics of the Atox test setup

the slit. The vertical probe reading gives a profile of ion emission along the slit length, i.e. an indication of the uniformity of ion emission along the slit (or lack thereof). The positioning system has an angular resolution of 0.9 deg and covers a total angle of 106.2 and 133.2 deg for the vertical and horizontal probes, respectively.

Test procedure and conditions

The Atox test was conducted according to the following procedure:

1. The thruster was operated at a fixed voltage level (5 kV emitter voltage, -2 kV accelerator voltage). The ion beam profiles were acquired, with special regard to vertical probe scans, showing emission distribution along the slit.
2. The thruster was switched off and let cool down until cesium was solid. The Atox source was switched on at fixed oxygen mass flow and magnetron current.
3. The thruster was exposed to atomic oxygen for 8 days continuously, keeping cesium solid (“first period”). The emitter temperature never exceeded 23 °C.
4. The atomic oxygen source was switched off and the thruster was fired at the same voltage levels as before. Ion beam profiles were recorded.
5. The thruster was switched off and kept at the nominal operating temperature, about 35 °C. In this condition, cesium is liquid. The Atox source was switched again.
6. The thruster was exposed to atomic oxygen for 8 days continuously, keeping cesium liquid (“second period”).

7. The atomic oxygen source was switched off. The thruster was fired at the previously defined voltage levels. Ion beam profiles were recorded.

Test conditions during both periods of source operation remained stable. In particular:

- laboratory (ambient) temperature was maintained between 20 and 21 °C;
- magnetron current was kept constant at 60 mA;
- source temperature remained between 92 and 105 °C;
- vacuum chamber pressure remained constant at $4 \cdot 10^{-4}$ mbar, showing regularity of oxygen flow and pumping speed;
- atomic oxygen flux was measured daily.

Measured values of atomic oxygen flux are shown in figure 11. The mean value was $1.5 \cdot 10^{16}$ atoms·s/cm² during the first period and $1.6 \cdot 10^{16}$ atoms·s/cm² during the second period. It is worth noting that chamber pressure before operation of the atomic oxygen source was around 10^{-7} mbar. Background pressure was therefore composed mainly (>99 %) by molecular oxygen.

The environmental conditions throughout the test were far worse than anything that could ever be experienced in the Low Earth Orbit environment. In fact, molecular oxygen was obviously the main constituent of the background atmosphere during the Atox test. Total pressure during the test was 2 orders of magnitude larger than the maximum total pressure expected in reference conditions ($1.5 \cdot 10^{-6}$ mbar, see Table 1). In addition to that, this pressure was contributed almost 100% by the highly reactive O₂ species, contrary to what occurs in space at 200 km where benign species (H, N₂ and Ar) have a significant share of the total pressure. Thus, the working conditions have to be regarded as extremely conservative.

In these conditions, for each exposure period, the total atomic oxygen fluence at the slit was:

$$N_O^{tot} = F_O \cdot t \cdot L_{slit} h_{slit} = 6.22 \cdot 10^{-18} \text{ atoms} = 1.7 \cdot 10^{-4} \text{ g}$$

where F_O is mean atomic oxygen flux on the slit, L_{slit} and h_{slit} are slit dimensions, t is total exposure time (192 h). The surface impingement rate for molecular oxygen, i.e. the number of molecules impinging on unit surface area per unit time, at test conditions, was:

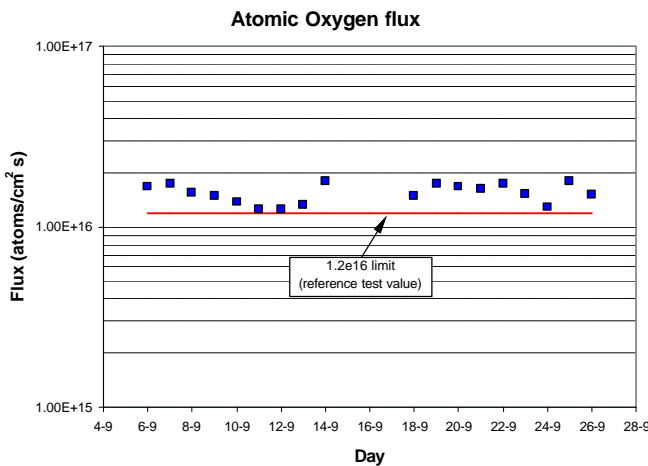


Figure 11 - Measured atomic oxygen flux during the Atox test

$$g = \frac{n\bar{c}}{6} = \frac{1}{6} \frac{pN_A}{RT} \sqrt{\frac{8kT}{\pi m}} = 7.2 \cdot 10^{16} \text{ molecules/cm}^2 \cdot \text{s}$$

where p is chamber pressure, N_A is the Avogadro number, R is the gas constant, T is chamber temperature, k is the Boltzmann constant and m is the O_2 molecular mass. The total oxygen dose received by the emitter slit, for each exposure period, was therefore not less than $1.77 \cdot 10^{-3}$ g. For comparison, the expected oxygen dose along the entire lifetime for the GOCE mission is:

$$N_O^{tot} = 1.63 \cdot 10^{19} \text{ atoms} = 4.3 \cdot 10^{-4} \text{ g}$$

The total amount of oxygen that the thruster could withstand without permanent deterioration of its performance was therefore four times higher than that

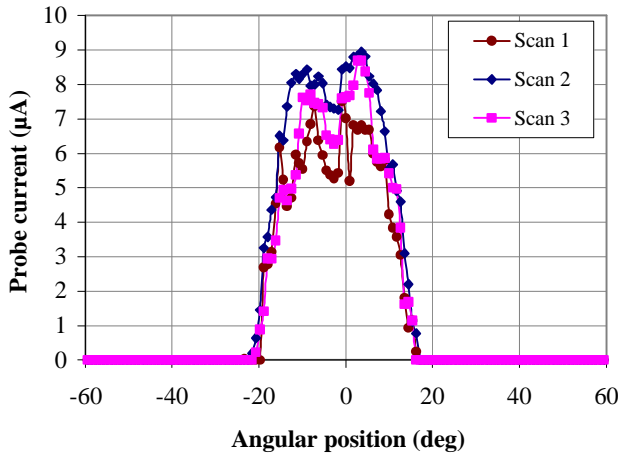
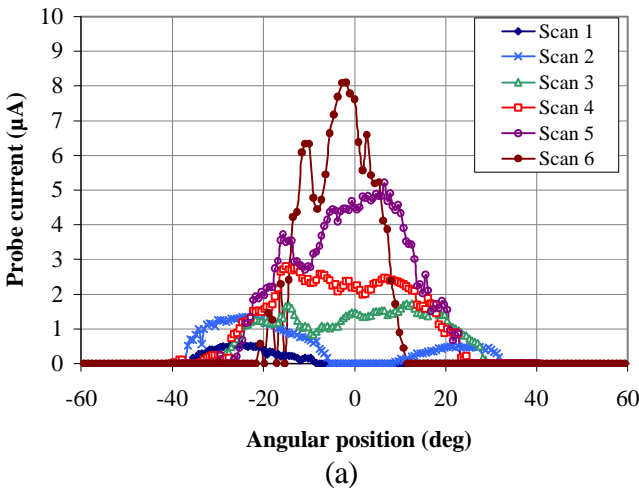


Figure 12 - Ion beam profiles along the slit before the Atox test



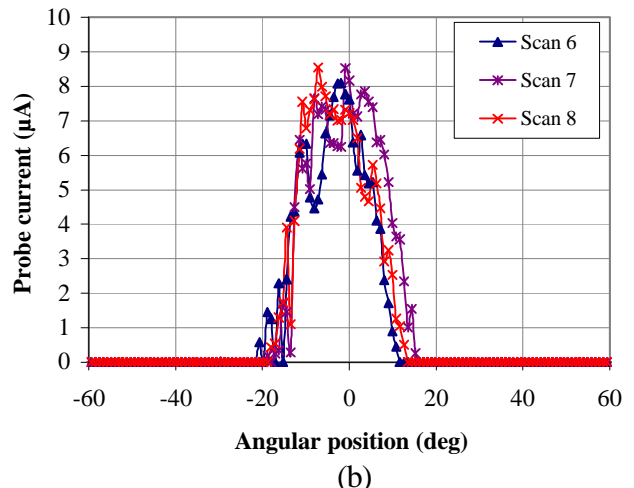
(a)

expected for the GOCE mission. As we show in the following section, this amount was tolerated both in hot and in cold emitter conditions.

Test results

A number of ion beam profiles at fixed voltage were acquired prior to atomic oxygen exposure. Three of these profiles, acquired with the vertical probe during the thruster first operational phase at a few minutes intervals, are plotted in fig. 12 and were used as a reference for thruster performance: any degradation like partial slit clogging would be revealed by a significant change in the profile shape.

Shortly after the source was turned off, the thruster was heated above the cesium melting temperature, at 39 °C. Total voltage was then raised up to 13 kV without ion emission. The temperature was then raised up to 49 °C. This time ion emission started immediately, at a voltage just above the previously recorded threshold (around 6.5 kV). Visual inspection clearly showed that emission started from one single site close to slit left border. This observation was confirmed by acquiring the ion beam profile. During the following few hours, both visual observation and profile acquisition showed the enlargement of the emitting area, starting with a second emission site on the opposite end of the slit and progressing to the whole slit length. Visual inspection also showed that some impurities, in yellow-brown colour, that had appeared along the slit during the non-operating period, were progressively removed by thruster operation. Thruster performance was fully restored, at the pre-Atox recorded level, after about 10 hours total operation at low total voltage (7 kV). Figure 13 shows vertical probe ion beam scans recorded at different times after Atox



(b)

Figure 13 - Ion beam profiles along the slit after the Atox test, first period

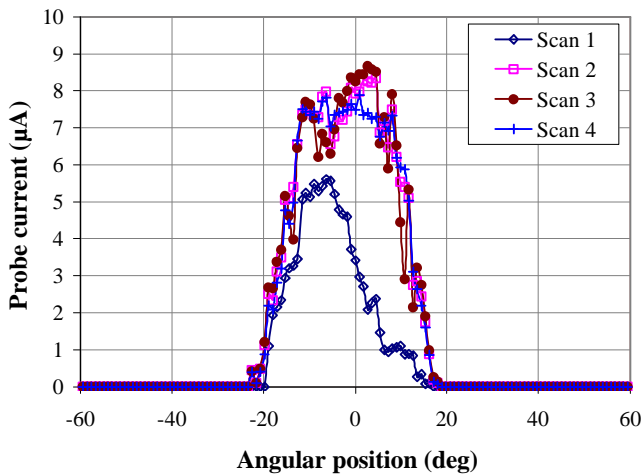


Figure 14 - Ion beam profiles along the slit after the Atox test, second period

exposure. The evolution of profiles in fig. 13-(a) clearly shows a more and more uniform emission and a raising current level, indicating that number of emission sites is increasing. The subsequent profiles in fig. 13-(b) show that the drained current reaches the same level that was previously recorded.

After the second period of atomic oxygen exposure (with hot emitter and liquid cesium), no difficulties were encountered in restarting the thruster at nominal operating temperature. Only some marginal degradation in current level and ion beam profile was observed immediately after restarting, and this degradation disappeared after about 1 hour operation. In fig. 14 below, all but “Scan 1” profile show that the

drained current and profile shape reach the pre-Atox exposure levels.

The restart difficulties recorded immediately after the end of the first exposure period were most probably due to the formation of a crust of cesium oxides that clogged the slit. This problem was easily overcome by heating at just 20 °C above the cesium melting point. The temperature rise caused the crust to break at some location, either under the action of internal stresses related to the temperature gradient, or as a consequence of differential expansion between the three neighbouring materials (pure cesium, cesium oxides, emitter stainless steel), or, again, due to capillary forces from the inside once the cesium was melted. Some cesium could then flow through the break in the crust and initiate ion emission, which resulted in progressive cleaning of the whole slit. An additional role might have been played by solubility of cesium oxides in pure cesium, that could help in crust breaking and removal. The presence of impurities on the slit, later removed by the restored ion emission, was probably due to the ejection of solid materials by the liquid cesium meniscus that is forced to reach the tip by capillary forces. It can be inferred that the adhesion forces between cesium oxides and emitter slit are quite faint and can be easily broken by thermal cycling or capillary action. An additional role might have been played by the solubility of cesium oxides in pure cesium, that could help in crust breaking and removal.

After the second atomic oxygen exposure, no problem was reported in restarting the thruster immediately after exposure. Initially, the thruster showed just

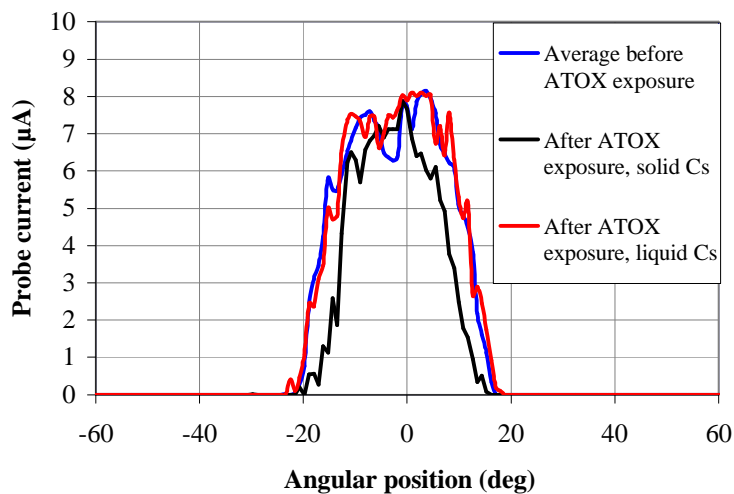


Figure 15 - Comparison of average ion beam profiles before and after exposure to atomic oxygen

some reduction in performance that was rapidly removed by normal operation. In this case, if any clogging was present, it clearly occurred on a portion of the slit only, letting emission restart at once from most of the slit length. This behaviour was probably due to solution in liquid cesium of cesium oxides and consequent removal of the same from the slit by some sort of diffusion process. Very fast performance recovery, and no visual observation of solid particles in front of the slit, also yields to assume that the oxides were more sparsely distributed.

Conclusions

The reported atomic oxygen compatibility test showed that exposure to a very intense atomic and molecular oxygen environment with cesium either in the solid or liquid state does not permanently affect the FEEP thruster performance. Momentary difficulties in restarting the FEEP thruster have been easily overcome by heating to a moderate temperature. Thruster performance before and after exposure to atomic oxygen and to a severe background oxygen atmosphere remains essentially identical: figure 14 shows the comparison between the mean ion beam profiles obtained before and after first and second exposure (data from figures 11, 12 and 13; for the sake of legibility, only lines interpolating the data points are shown). On the basis of the test results, we conclude that cesium-fed FEEP thrusters can operate safely in a very low Earth orbit environment.

Acknowledgments

This work was carried out in the frame of a contract of the European Space Agency. Part of the atomic oxygen source development was funded by the Italian Space Agency with a research grant. The authors are indebted to Mario Pessana of Alenia Aerospazio, Jan Wohlfart of Astrium GmbH, Gerard André and David Nicolini of ESA/ESTEC for their support, as well as to Marco Saviozzi and Leonardo Priami of Centropazio/Alta for their contribution to the experiments.

References

- [1] J. Mitterauer, "Contamination Test of a Cesium Field Ion Thruster", *J. Prop. Power Vol. 7, No. 3*, 1989.
- [2] A. Genovese, S. Marcuccio, D. Dal Pozzo, M. Andrenucci, "FEEP Thruster Performance at High Background Pressure", *IEPC-97-186*, 1997.

- [3] <http://www.spennis.oma.be/spennis/>
- [4] http://cyberbuzz.gatech.edu/asm_tms/phase_diagrams/
- [5] B. H. Mahan, "University Chemistry", *Addison-Wesley Publ. Comp.*, 1975.
- [6] P. Touzain, "Etude cinétique de l'oxydation des métaux alcalins par l'oxygène sec", *CEA-R 3301*, 1967.
- [7] D. R. Lide, *CRC Handbook of Chemistry and Physics*, 73rd edition, *CRC Press*, 1992 -1993.
- [8] <http://www.webelements.com>
- [9] *American Institute of Physics Handbook*, 2nd edition, New York, 1963.
- [10] M. R. Carruth, R. F. DeHaye, J. K. Norwood, A. F. Whitaker, "Method for Determination of Neutral Atomic Oxygen Flux", *Rev. Sci. Instrum.* 61 (4), April 1990.
- [11] J. W. Linette, D. G. H. Marsden, *Proc. Roy. Soc. London A234*, 489, 1956.
- [12] D. Peplinski *et al.*, "Satellite Exposure to Atomic Oxygen in Low Earth Orbit", in: *Introduction to Simulation of Upper Atmosphere Oxygen*, 1984.